Polymer Gel Templating Synthesis of Nanocrystalline Oxide Anodes

Dmitry G. Shchukin,*,† Aleksey A. Yaremchenko,‡ Mario G. S. Ferreira,‡ and Vladislav V. Kharton‡

Max-Planck Institute of Colloids and Interfaces, D14424 Potsdam, Germany, and Department of Ceramics and Glass Engineering, CICECO, University of Aveiro, 3810-193 Aveiro, Portugal

Received March 29, 2005. Revised Manuscript Received July 29, 2005

The synthesis of macroporous perovskite $La_{0.65}Sr_{0.3}CoO_{3-\delta}$ and spinel $NiCo_2O_4$ electrodes was achieved by infiltration of $La_{0.65}Sr_{0.3}CoO_{3-\delta}$ and $NiCo_2O_4$ colloid solutions inside a polymer gel template followed by calcination at 1100 °C to obtain single-phase materials. Resulting inorganic materials are porous and have a high specific surface area up to 90 $m^2\ g^{-1}$, average pore diameter ∼450 nm, and 20−50 nm particle size. The structure of inorganic networks shows obvious similarities to the initial polymer gel network. Porous $NiCo_2O_4$ spinel can also be obtained from a precursor salt solution, whereas $La_{0.65}Sr_{0.3}CoO_{3-\delta}$ perovskite formed after template impregnation from a precursor salt solution has a dense structure with a low specific surface area. Macroporous inorganic networks exhibit high electrocatalytic activity toward oxygen evolution from alkaline water solutions with the efficiency substantially better than that of the film electrodes having a similar composition. The highest activity was observed for the $La_{0.65}Sr_{0.3}CoO_{3-\delta}$ perovskite network.

Introduction

Developments of highly active oxide electrodes for the electrochemical evolution and reduction of oxygen in alkaline media are of considerable interest for numerous technological applications including secondary metal−air batteries, hydrogen production by water electrolysis, low-temperature fuel cells, electrosynthesis, and metal processing.[1−8] Two promising groups of materials, which possess sufficient conductivity and can be applied as bifunctional electrodes with a substantial performance for both these processes, are perovskite-type compounds based on lanthanum−strontium cobaltites, $(La,Sr)CoO_{3-\delta}$, and mixed Ni−Co oxides with a spinel structure.[5,6] The search for the most active composition should, however, accompany the elaboration of novel processing technologies enabling the synthesis of nanocrystalline materials with a high surface concentration of catalytically active centers and a large surface area as well as the optimization of the electrode microstructure to avoid mass transport limitations during the electrochemical reactions.[1]

Highly porous inorganic materials can be fabricated by template synthesis employing organic structures of different natures (e.g., polymer gels,[9,10] block-copolymers,[11,12] liquid crystals,[13] membranes,[14] wood,[15] and fibers[16]). The properties of the final inorganic network including outer and inner surface area, pore system, and size distribution of the composing particles can be predetermined by the characteristics of the organic template that acts as a scaffold around which the desired inorganic material is formed. The final network can be either an inverse replica or a hollow replica depending on whether complete cast or coating was achieved.[17−20] Templated inorganic materials are promising candidates for catalytic application due to their high porosity, surface availability, and large specific surface area. These properties can considerably increase the efficiency of the reaction (e.g., in electrocatalytic processes) without the increase in current density and the consequent enhancement of electrode corrosion that is important for anodic reactions.

* Corresponding author. E-mail: Dmitry.Shchukin@mpikg.mpg.de.
† Max-Planck Institute of Colloids and Interfaces.
‡ University of Aveiro.

(1) Kinoshita, K. *Electrochemical oxygen technology*; Wiley: New York, 1992.
(2) Singh, R. N.; Lal, B. *Int. J. Hydrogen Energy* **2002**, *27*, 45−55.
(3) Kahoul, A.; Hammouche, A.; Poillerat, G.; De Doncker, R. W. *Catal. Today* **2004**, *89*, 287−291.
(4) Bockris, J. O.; Otagawa, T. *J. Electrochem. Soc.* **1984**, *131*, 290−302.
(5) Sviridov, D. V.; Kovalevsky, A. V.; Kharton, V. V.; Naumovich, E. N.; Frade, J. R. *Mater. Sci. Forum* **2005**, *498*, 115−119.
(6) Suffredini, H. B.; Cerne, J. L.; Crnkovic, F. C.; Machado, S. A. S.; Avaca, L. A. *Int. J. Hydrogen Energy* **2000**, *25*, 415−423.
(7) De Chialvo, M. R. G.; Chialvo, A. C. *Electrochim. Acta* **1993**, *38*, 2247−2255.
(8) Hu, C. C.; Lee, Y. S.; Wen, T. C. *Mater. Chem. Phys.* **1997**, *48*, 246−254.
(9) Schattka, J. H.; Shchukin, D. G.; Jia, J.; Antonietti, M.; Caruso, R. A. *Chem. Mater.* **2002**, *14*, 5103−5108.
(10) Caruso, R. A.; Giersig, M.; Willig, F.; Antonietti, M. *Langmuir* **1998**, *14*, 6333−6336.
(11) Zhao, D.; Feng, J.; Huo, Q.; Melosh, N.; Fredrickson, G. H.; Chmelka, B. F.; Stucky, G. D. *Science* **1998**, *279*, 548−552.
(12) Smarsly, B.; Polarz, S.; Antonietti, M. *J. Phys. Chem. B* **2001**, *105*, 10473−10483.
(13) Beck, J. S.; Vartuli, J. C.; Roth, W. J.; Leonowicz, M. E.; Kresge, C. T.; Schmitt, K. D.; Chu, C. T. W.; Olson, D. H.; Sheppard, E. W.; McCullen, S. B.; Higgins, J. B.; Schlenker, J. L. *J. Am. Chem. Soc.* **1992**, *114*, 10834−10843.
(14) Martin, C. R. *Chem. Mater.* **1996**, *8*, 1739−1746.
(15) Cao, J.; Rambo, C. R.; Sieber, H. *J. Porous Mater.* **2004**, *11*, 163−172.
(16) He, J. H.; Kunitake, T.; Watanabe, T. *Chem. Commun.* **2005**, 795−796.
(17) Ozin, G. A.; Oliver, S. *Adv. Mater.* **1995**, *7*, 931−943.
(18) Mann, S.; Archibald, D. D.; Didymus, J. M.; Heywood, B. R.; Meldrum, F. C.; Reeves, N. J. *Science* **1993**, *261*, 1286−1292.
(19) Vettraino, M.; Ye, B.; He, X.; Antonelli, D. M. *Aust. J. Chem.* **2001**, *54*, 85−88.
(20) Han, B. H.; Antonietti, M. *J. Mater. Chem.* **2003**, *13*, 1793−1796.

10.1021/cm050672u CCC: $30.25
Published on Web 08/27/2005

Al_2O_3- and SiO_2-based materials attract particular attention for chemical catalysis. The most prominent MCM-41 modified by different compounds (Pt, Pd, Cr_2O_3, etc.) is active in NO reduction, Suzuki cross-linking, oil cracking, and syngas production.[21,22] Other porous oxide materials with high catalytic efficiency are ceria,[23] zirconia,[24] niobium oxide,[25] iron oxides,[26] and titania.[27] Porous titanium dioxide showed prominent photocatalytic properties both along (photooxidation of phenols) and in combination with the second oxide (ZrO_2, In_2O_3).[9,28−30] Several attempts were made to synthesize conductive porous materials, especially metals, for electrocatalytic applications: block-copolymer templated iron, cobalt−nickel and iron−cobalt alloys,[31] DNA templated noble metals,[32] and mesoporous carbon.[33] However, there is no information up to date regarding the possibility of employing a templating approach for the fabrication of porous inorganic materials that have conductivity sufficient for electrocatalytic applications and require high-temperature annealing to obtain a single phase without amorphous components. The temperature range previously used in template synthesis was within 350−800 °C, which is enough to remove the template and to crystallize most of the oxides. The main drawback of annealing at elevated temperatures (above 800 °C) is the increase of the particle size followed by the decrease of the specific surface area resulting from destruction of the inner porous structure.

Here, we explore the applicability of the template protocol for obtaining porous networks of perovskites and spinels at temperatures above 1000 °C. $La_{0.65}Sr_{0.3}CoO_{3-\delta}$ with a perovskite-type structure and a $NiCo_2O_4$ spinel were tested as model compounds active for electroassisted oxygen oxidation at pH > 8. $La_{0.65}Sr_{0.3}CoO_{3-\delta}$ was selected as a composition with high electrochemical performance in oxygen evolution from water and sufficient stability in alkaline media.[5] $NiCo_2O_4$ is also known as an active and stable bifunctional catalyst for oxygen evolution in alkaline media and for electrochemical oxidation of alcohols and amines.[6−8] Note that the electrocatalytic behavior of $Ni_{1-x}Co_xO_z$ mixed oxides in the intermediate range of nickel content is predominantly governed by the performance of a stoichiometric $NiCo_2O_4$ spinel, although an excess of NiO may even increase the electrochemical activity.[7,8]

The acrylamide/glycidyl methacrylate polymer gel was used as a templating agent. This template can easily be prepared, and the preparation method allows flexibility in the porous structure, pH stability, and surface functionality.[9] The polymer gel has previously been studied as a template material for the formation of macroporous titania and zirconia.[9,28] A micron-scale pore diameter of the gel is a necessary condition to provide effective reagent exchange inside the network and exclusion of the oxygen bubbles from the network volume formed during electrochemical H_2O oxidation.[1]

Experimental Procedures

Materials. Tween 60 (polyoxoethylene (20) sorbitan monostearate), glycidyl methacrylate, ethylene glycol dimethacrylate, acrylamide, and potassium persulfate were used for preparation of the polymer gel. To synthesize $La_{0.65}Sr_{0.3}CoO_{3-\delta}$ and $NiCo_2O_4$ nanoparticles, $Na_3Co(NO_3)_6$, $Sr(NO_3)_2$, $La(NO_3)_3$, $Ni(NO_3)_2{\cdot}6H_2O$, NaOH, and ethylene glycol were utilized. All chemicals were purchased from Aldrich and used without additional purification. The water was obtained from a three-stage Millipore Milli-Q Plus 185 purification system and had a resistivity higher than 18 MΩ cm.

Preparation of Initial Sols. $La_{0.65}Sr_{0.3}CoO_{3-\delta}$ and $NiCo_2O_4$ colloids were obtained by hydrolysis of the corresponding salts according to the procedure adapted from refs 34−36. A total of 0.4 g of $Na_3Co(NO_3)_6$ was dissolved in 20 mL of H_2O; then, 80 μL of ethylene glycol, 0.062 g of $Sr(NO_3)_2$, and 0.28 g of $La(NO_3)_3$ were added into the solution one after another to achieve a La/Sr/Co molar ratio equal to 0.65:0.3:1. For $NiCo_2O_4$ sol preparation, 20 mL of the precursor solution containing 0.4 g of $Na_3Co(NO_3)_6$ + 0.144 g of $Ni(NO_3)_2{\cdot}6H_2O$ + 80 μL of ethylene glycol was taken. Precursor solutions were hydrolyzed by 1 M NaOH under vigorous stirring at room temperature. The pH value of the solution after hydrolysis should not exceed 10. Resulting precipitates were washed 3 times with water by centrifugation. Afterward, precipitated nanoparticles were redispersed by the addition of a stabilizer (ethylene glycol) and ultrasonic treatment (Bandelin SONOPLUS HD200 equipped with a probe horn). Ready-to-use colloid suspensions had concentrations of 3.1 g L^{-1} ($La_{0.65}Sr_{0.3}CoO_{3-\delta}$), 3.35 g L^{-1} ($NiCo_2O_4$), and an average diameter of 8 and 10 nm, respectively. Colloidal solutions are stable at room temperature for approximately 2 weeks; thereafter, rapid agglomeration is observed.

Formation of Polymer Gel Template. Synthesis of the polymer gel followed the procedure previously reported in ref 9: the structure-directing surfactant (Tween 60, 40 g) was mixed with water (80 mL) with stirring. Then, monomers (10 g of acrylamide and 10 g of glycidyl methacrylate) and a cross-linker (4 g of ethylene glycol dimethacrylate) were added. Stirring continued until a homogeneous solution was obtained. After the addition of an initiator (1 g of potassium persulfate), the mixture was poured into test tubes and placed in an oil bath at 55 °C for 24 h to complete polymerization. The resulting gel was cut into disks and cleaned by Soxhlet extraction with ethanol for 1 week to remove the structure-directing surfactant.

(21) Sobczak, I.; Ziolek, M.; Nowacka, M. *Microporous Mesoporous Mater.* **2005**, *78*, 103−116.
(22) Corma, A.; Das, D.; Garcia, H.; Leyva, A. *J. Catal.* **2005**, *229*, 322−331.
(23) Deshpande, A. S.; Pinna, N.; Smarsly, B.; Antonietti, M.; Niederberger, M. *SMALL* **2005**, *1*, 313−316.
(24) Brezesinski, T.; Antonietti, M.; Groenewolt, M.; Pinna, N.; Smarsly, B. *New. J. Chem.* **2005**, *29*, 237−242.
(25) Hiyoshi, M.; Lee, B.; Lu, D.; Hara, M.; Kondo, J. N.; Domen, K. *Catal. Lett.* **2004**, *98*, 181−186.
(26) Srivastava, D. N.; Perkas, N.; Gedanken, A.; Felner, I. *J. Phys. Chem. B* **2002**, *106*, 1878−1883.
(27) Pizzio, L. P. *Mater. Lett.* **2005**, *59*, 994−997.
(28) Shchukin, D. G.; Schattka, J. H.; Antonietti, M.; Caruso, R. A. *J. Phys. Chem. B* **2003**, *107*, 952−957.
(29) Shchukin, D. G.; Caruso, R. A. *Chem. Mater.* **2004**, *16*, 2287−2292.
(30) Deshpande, A. S.; Shchukin, D. G.; Ustinovich, E.; Antonietti, M.; Caruso, R. A. *Adv. Funct. Mater.* **2005**, *15*, 239−245.
(31) Abes, J. I.; Cohen, R. E.; Ross, C. A. *Mater. Sci. Eng., C* **2003**, *23*, 641−650.
(32) Brunner, J.; Mokhir, A.; Kraemer, R. *J. Am. Chem. Soc.* **2003**, *125*, 12410−12411.
(33) Hinderling, C.; Keles, Y.; Stockli, T.; Knapp, H. E.; de los Arcos, T.; Oelhafen, P.; Korczagin, I.; Hempenius, M. A.; Vancso, G. J.; Pugin, R. L.; Heinzelmann, H. *Adv. Mater.* **2004**, *16*, 876−879.
(34) Poznyak, S. K.; Kokorin, A. I.; Kulak, A. I. *J. Electroanal. Chem.* **1998**, *442*, 99−105.
(35) Chandler, C. D.; Roger, C.; Hampden-Smith, M. J. *Chem. Rev.* **1993**, *93*, 1205−1241.
(36) Niederberger, M.; Pinna, N.; Polleux, J.; Antonietti, M. *Angew. Chem., Int. Ed.* **2004**, *43*, 2270−2273.

Templating Procedure. Pieces of gel template were immersed in the aqueous colloidal solutions of $La_{0.65}Sr_{0.3}CoO_{3-\delta}$ and $NiCo_2O_4$ and stored at room temperature for 10 days. A period of 10 days was chosen for soaking all samples to achieve reproducibility and homogeneity in the final inorganic material. A lower immersion time leads to the incomplete loading of the template with inorganic nanoparticles, whereas a higher immersion time is not possible due to the agglomeration of the initial sols. To compare the efficiency of the inorganic network formation using as-prepared nanoparticles, a polymer template was also impregnated by the solution of the corresponding precursor salts (1.34 g of $Co(NH_3)_6Cl_3$ + 0.316 g of $Sr(NO_3)_2$ + 1.41 g of $La(NO_3)_3$ in 50 mL of H_2O or 1.34 g of $Co(NH_3)_6Cl_3$ + 0.73 g of $Ni(NO_3)_2 \cdot 6H_2O$ in 50 mL of H_2O) for 10 days. After impregnation, all polymer/inorganic composites were rinsed with water and dried for 3 h at 60 °C. The template material was removed by heating all samples until 1100 °C in argon flow with a ramp rate of 4 °C min^{-1} followed by annealing at 1100 °C in air flow for 10 h. This calcination procedure was chosen to achieve complete formation of perovskite and the spinel phase, which occurs at the temperatures above 1000 °C.[5]

Characterization. To dry the polymer gel sample for electron microscopy, a freeze-dryer, Lyovac GT2 from FINN-AQUA GbmH, was used. The scanning electron microscopy (SEM) analysis was performed to investigate both the original gel structure and that of the resulting networks using a Gemini Leo 1550 instrument operating at 3 keV. The samples were broken to expose fresh surfaces and mounted onto carbon-coated stubs before gold sputter coating. To view the interior of the network structure, the samples were embedded in poly(methyl methacrylate) capsules, and then ultrathin sections (30−100 nm in thickness) were obtained by a Leica ultracut UCT ultramicrotome. Carbon or noncoated copper grids were used to support the thin sections, and a Zeiss EM 912 Omega transmission electron microscope (TEM) was employed for analysis.

To determine the weight percent of inorganic to organic material after calcination, thermogravimetric analysis (TGA) was conducted using a Netzsch TG 209 apparatus. Specific surface area and porosity of the inorganic networks were measured on Micromeritics Tristar instrument (BET analysis after N_2 adsorption) and on Micromeritics Mercury Porosimeter, respectively. The crystal structure of the inorganic networks was determined from wide-angle X-ray scattering (WAXS), Enraf-Nonius PDS-120. A Perkin-Elmer Analyst 700 atomic absorbance spectrometer was employed to estimate the element ratio in the networks.

Investigation of the electrocatalytic activity of inorganic networks was carried out in a standard two-compartment three-electrode cell with a platinum counter-electrode and an Ag/AgCl/KCl (saturated) electrode as a reference electrode (+0.201 V vs standard hydrogen electrode). All potentials were set with respect to this reference electrode and were controlled by an Autolab PGSTAT30 potentiostat. Inorganic networks were attached to the working electrode (Pt) spindle by conducting Ag-glue paste to provide electric contact, and then, this contact was isolated from the electrolyte solution (1 M NaOH).

Results and Discussion

Materials employed as templates should have a porous structure stable on the impregnation and drying stages. Furthermore, the volume of the template should be accessible for precursor intercalation from a surrounding solution. The template must be completely removed without interaction with a formed inorganic replica by calcination or dissolution. The template material chosen for this study is a polymer gel composed of acrylamide and glycidyl methacrylate cross-linked by ethylene glycol dimethacrylate. It has a porous globular structure with a homogeneous pore distribution in the whole volume (Figure 1). The specific surface area of the freeze-dried template, obtained from BET analysis, is 32 m^2 g^{-1}. The polymer gel is chemically stable and maintains a native porous structure during impregnation and drying. Glycidyl groups of the gel are almost completely hydrolyzed to two chelating hydroxy groups that promote good binding of the nanoparticles and salt precursors.

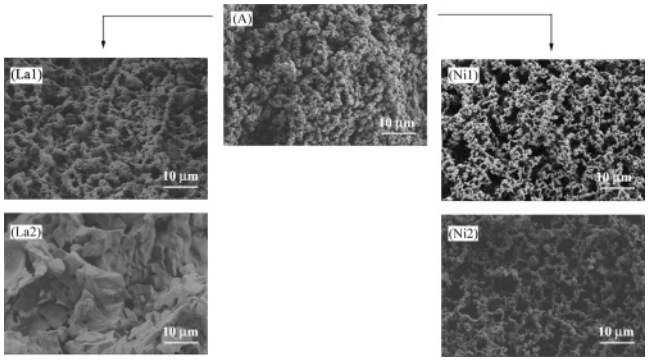

Figure 1. SEM images of (a) the initial freeze-dried template gel and resulting inorganic networks prepared from preformed sols (La1 for $La_{0.65}Sr_{0.3}CoO_{3-\delta}$ and Ni1 for $NiCo_2O_4$) and from precursor solutions of corresponding salts (La2 for $La_{0.65}Sr_{0.3}CoO_{3-\delta}$ and Ni2 for $NiCo_2O_4$).

There are two general mechanisms of forming inorganic network replicas: coating, where preformed inorganic nanoparticles adsorb inside the template material covering inner walls, and casting, where a solution of the inorganic precursor fills the pore volume and formation of the inorganic networks starts within the pore volume. Here, we explore the possibility of preparing electrocatalytic perovskite and spinel networks by both mechanisms using either preformed nanoparticles or salt solutions. The polymer template was removed by calcination at 1100 °C in the presence of oxygen that resulted in pyrolysis of the organic scaffold and formation of the perovskite or spinel phase. All the samples underwent the same thermal treatment to obtain a template-free inorganic network. $Co(NH_3)_6Cl_3$ was used in the precursor salt solution as a source of cobalt because the use of $Na_3Co(NO_3)_6$ for casting results in a partial oxidation of the template gel, destroying its native structure.

The resultant inorganic structures are visualized by scanning electron microscopy as shown in Figure 1. The formation of homogeneous porous inorganic networks was achieved for $La_{0.65}Sr_{0.3}CoO_{3-\delta}$, $NiCo_2O_4$ prepared from the preformed colloids (samples La1 and Ni1, respectively), and $NiCo_2O_4$ obtained from the $Co(NH_3)_6Cl_3/Ni(NO_3)_2$ precursor solution (sample Ni2). These networks are similar to the initial structure of the template. The inorganic materials obtained after calcination have lower geometric dimensions as compared to the initial template. The shrinkage is ~28% for the La1 and Ni1 networks and smaller, ~18%, for the Ni2 sample. The shrinkage is comparable to that observed before the templating of three-dimensional structures.[28,37] The shrinkage is caused by incomplete filling of the template

(37) Breulmann, M.; Davis, S. A.; Mann, S.; Hentze, H.-P.; Antonietti, M. *Adv. Mater.* **2000**, *12*, 502−507.

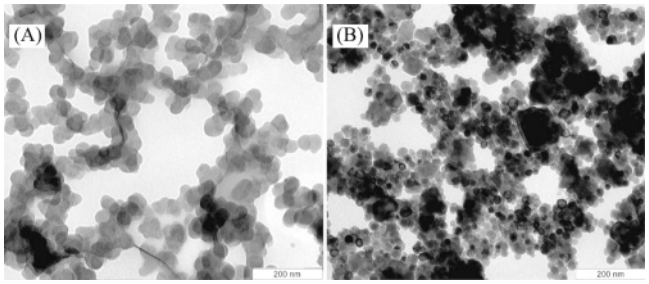

Figure 2. TEM images of the ultramicrotomed $La_{0.65}Sr_{0.3}CoO_{3-\delta}$ (a, La1 sample) and $NiCo_2O_4$ (b, Ni1 sample) networks. Samples were prepared from preformed sols.

pores by inorganic material and is more obvious while using as-prepared colloidal solutions because the concentration of inorganic components is considerably lower (<1%) as compared to the salt solutions. Hence, the whole pore volume is not completely filled with inorganic material resulting in a coating of the template walls and related shrinkage during drying and calcination. However, the amount of adsorbed nanoparticles is enough to maintain an initial template structure during formation of the perovskite or spinel phases. A porous inorganic network is formed inside the polymer gel template starting from 500 °C;[9,28] a further increase in the temperature up to 1100 °C provokes the crystallization followed by particle growth from 8 to 40 nm.

The use of a $Co(NH_3)_6Cl_3/Sr(NO_3)_2/La(NO_3)_3$ precursor solution to prepare the $La_{0.65}Sr_{0.3}CoO_{3-\delta}$ network was unsuccessful; only dense, compact structures were formed (Figure 1, sample La2). A similar phenomenon was previously observed for In_2O_3, Fe_2O_3, etc.[29] and can be explained by densification of the corresponding oxide structures obtained from precursor salts at the calcination step followed by intense agglomeration of colloid particles. Such densification is typical for multicomponent oxides containing the materials used to form dense oxide layers such as Al_2O_3 or La_2O_3.[38,39] Moreover, a three-component structure of the $La_{0.65}Sr_{0.3}CoO_{3-\delta}$ (three different oxides are to be combined in one particle during calcination of the precursor salts inside the gel matrix) could also reduce the possibility of obtaining a porous replica from salts during template calcination and increase the agglomeration of the particles. A variation in the La/Sr/Co ratio in the precursor solution did not affect the observed dense structure.

The nanoparticles forming the final $La_{0.65}Sr_{0.3}CoO_{3-\delta}$ and $NiCo_2O_4$ network structures are seen on microtomed slices in Figure 2. TEM analysis showed a porous structure of metal oxide networks obtained. This structure is quite similar to the structures reported previously for titania and zirconia networks annealed at 500 °C.[28,29] Large 200−400 nm pores originating from initial template structures and small 20−50 nm ones formed between nanoparticles are observed. The TEM images confirmed the porosity throughout the whole volume of the networks. Nanoparticles of both $La_{0.65}Sr_{0.3}CoO_{3-\delta}$ and $NiCo_2O_4$ are quite monodisperse; they are smaller for $NiCo_2O_4$ (∼30 nm) as compared to

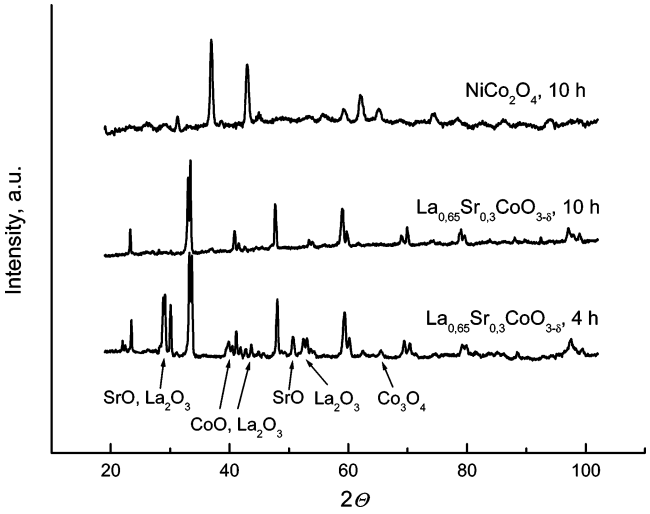

Figure 3. X-ray scattering patterns of the $NiCo_2O_4$ network annealed at 1100 °C for 10 h and of $La_{0.65}Sr_{0.3}CoO_{3-\delta}$ networks annealed at 1100 °C for 4 and 10 h.

Table 1. Properties of Inorganic Networks Prepared from Sols and Salt Solutions

Material	SA ($m^2\ g^{-1}$)[a]	wt % inorganic[b]
initial template gel	32	0
$La_{0.65}Sr_{0.3}CoO_{3-\delta}$ (sol)	85	9
$La_{0.65}Sr_{0.3}CoO_{3-\delta}$ (soln)	6	25
$NiCo_2O_4$ (sol)	90	10
$NiCo_2O_4$ (soln)	44	15

[a] Obtained from N_2 adsorption measurements. [b] Obtained from TGA of the impregnated template structures.

$La_{0.65}Sr_{0.3}CoO_{3-\delta}$ (∼40 nm), but $NiCo_2O_4$ particles are more aggregated. The $NiCo_2O_4$ sample prepared from the precursor salt solution has a similar porous structure and size of particles as $NiCo_2O_4$ obtained from a preformed sol (results not shown).

X-ray diffraction (XRD) data confirm the high crystallinity of the final inorganic networks. Elemental analysis of the resulting solid material showed a La/Sr/Co ratio equal to 0.63:0.31:1.02, which is in close agreement to the La/Sr/Co ratio in the initial colloid solutions (0.65:0.30:1.00). The same information was obtained for the $NiCo_2O_4$ network: according to elemental analysis, the Ni/Co ratio for solid material is 0.98:2.01. XRD revealed the presence of a pure perovskite phase for the $La_{0.65}Sr_{0.3}CoO_{3-\delta}$ network and a pure spinel phase for the $NiCo_2O_4$ networks annealed at 1100 °C in air flow for 10 h (Figure 3). However, if the sample is annealed at 1100 °C for only 4 h, the perovskite phase coexists with several phase impurities (Figure 3). Therefore, high temperature and long calcination time are ultimate conditions for fabrication of the single-phase perovskite or spinel structure. Annealing the initial $La_{0.65}Sr_{0.3}CoO_{3-\delta}$ and $NiCo_2O_4$ sols without templating under the same conditions resulted in the formation of the same crystal phases.

High annealing temperature provokes particle growth, which is followed by the decrease of the specific surface area. However, the resulting $La_{0.65}Sr_{0.3}CoO_{3-\delta}$ and $NiCo_2O_4$ have a specific surface area higher than that of the initial organic template (see Table 1), and its values are dependent on the type of the inorganic network as well as on the impregnation conditions. The highest specific surface area

(38) Sanchez-Lopez, J. C.; Fernandez, A. *Mater. Sci. Forum* **1998**, *269*, 827−832.
(39) Kang, S. W.; Rhee, S. W. *J. Electrochem. Soc.* **2002**, *149*, C345−C348.

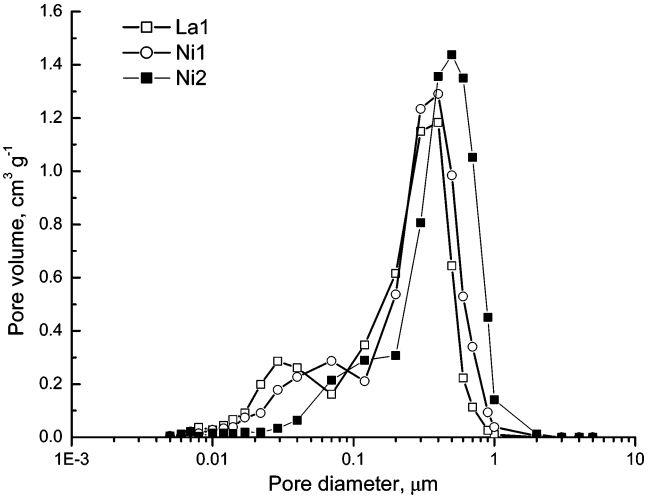

Figure 4. Mercury intrusion analysis of the networks prepared from preformed sols (La1 for $La_{0.65}Sr_{0.3}CoO_{3-\delta}$ and Ni1 for $NiCo_2O_4$) and of $NiCo_2O_4$ (Ni2 sample) prepared from a precursor solution.

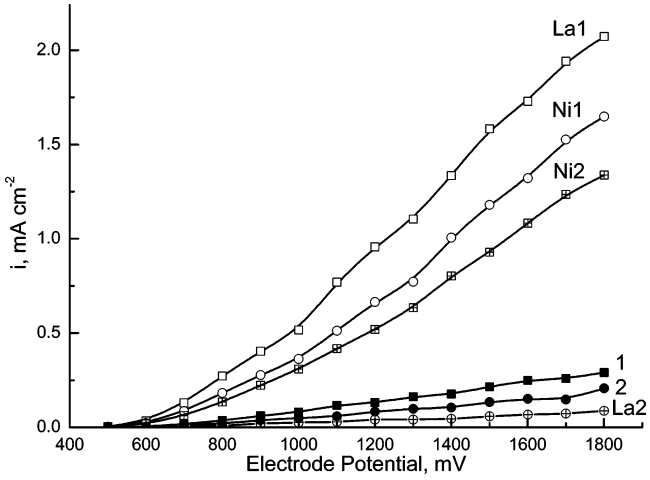

Figure 5. Oxygen electrooxidation from 1 M NaOH aqueous solution on porous (La1) $La_{0.65}Sr_{0.3}CoO_{3-\delta}$ and (Ni1) $NiCo_2O_4$ electrodes prepared from preformed sols; porous (Ni2) $NiCo_2O_4$ and dense (La2) $La_{0.65}Sr_{0.3}CoO_{3-\delta}$ electrodes prepared from corresponding precursor salt solutions; and (1) $La_{0.65}Sr_{0.3}CoO_{3-\delta}$ and (2) $NiCo_2O_4$ electrode pellets taken for comparison. Anodic current is normalized to the geometric surface area of the electrodes.

was found for $NiCo_2O_4$ prepared from preformed nanoparticles; the surface area of $La_{0.65}Sr_{0.3}CoO_{3-\delta}$ from preformed nanoparticles is slightly (5%) lower. Comparison of these values with a specific surface area for $NiCo_2O_4$ prepared from salts indicates a 50% decrease, while in the case of the unsuccessful La2 sample, only 6 $m^2\ g^{-1}$ was measured. The latter proves a dense structure of $La_{0.65}Sr_{0.3}CoO_{3-\delta}$ prepared from corresponding precursor salts as observed by SEM (Figure 1).

The pore size distributions from mercury intrusion measurements of final inorganic networks are shown in Figure 4. The analysis gives a bimodal pore distribution: the large pores (dominated at 340−530 nm) are those from the original polymer gel structure, which is because the shrinkage during calcination became smaller[9] and small pores (dominated at 25−50 nm) formed upon removal of the polymer scaffold. Bimodal pore distribution corresponds to the pore sizes obtained from both TEM and N_2 sorption analysis. Porous structures of $La_{0.65}Sr_{0.3}CoO_{3-\delta}$ and $NiCo_2O_4$ prepared from preformed nanoparticles are similar to each other. The size of both large and small pores is significantly increased for $NiCo_2O_4$ prepared from a precursor solution. This can be explained by in situ formation of the $NiCo_2O_4$ replica from precursor salts loaded in the template during drying and calcination resulting in bigger particles with a lower specific surface area (Table 1) and larger distance between each other. Moreover, higher loading of the template with the inorganic material from a precursor solution reveals lower shrinkage upon calcination, preserving the original pore size of the template better than for the La1 and Ni1 samples. Also, from the data obtained by TGA (Table 1), a higher weight percentage of the inorganic material after template removal is observed for the porous structures synthesized from precursor salts, indicating a more pronounced infiltration of the template from the salt solution than from the colloid solution. Similar inorganic content of the template gel loaded from $La_{0.65}Sr_{0.3}CoO_{3-\delta}$ or $NiCo_2O_4$ sols can be explained by the same infiltration conditions and parameters for both colloids that have approximately equal particle size and concentration. As reported previously,[28,29,37] the quantity of the inorganic material introduced inside the template from a preformed colloidal solution is mostly affected by particle size and concentration of the solution.

As known from literature,[5−8] the $La_{0.65}Sr_{0.3}CoO_{3-\delta}$ and $NiCo_2O_4$ phases possess high electrocatalytic activity in anodic processes. An oxygen evolution reaction in aqueous alkali solution was chosen to assess the activity of the prepared inorganic networks. Electrochemical experiments for all samples were performed potentiostatically in 1 M NaOH electrolyte. As an analytical signal, the value of the diffusion current at a fixed potential was taken with the potential step equal to 100 mV in an anodic direction. All electrodes were stable in 1 M NaOH and revealed no electrocorrosion at potentials less than +2.0 V versus the Ag/AgCl/KCl (saturated) electrode. Ceramic pellets of $La_{0.65}Sr_{0.3}CoO_{3-\delta}$ or $NiCo_2O_4$ formed by calcination of corresponding powders at 1100 °C (detailed description of their properties can be found in refs 1 and 5) were employed to compare electrocatalytic activities of the final inorganic networks.

All templated materials revealed a drastic increase in the oxygen evolution efficiency as compared to the corresponding dense electrodes (Figure 5). The most pronounced effect was observed for porous $La_{0.65}Sr_{0.3}CoO_{3-\delta}$ which is approximately 10 times more effective than the respective dense ceramic electrode. In general, the electrode performance is strongly correlated with the specific surface area of the samples. Samples with the highest surface area prepared from preformed sols (La1, Ni1) are most effective in oxygen evolution; a lower surface area of $NiCo_2O_4$ obtained from the precursor salt solution decreases the rate of oxygen oxidation, while nonporous $La_{0.65}Sr_{0.3}CoO_{3-\delta}$ prepared from precursor salt solution is even less active than the corresponding dense pellets probably due to local compositional inhomogeneities.

Another important comment is that the activity of templated $La_{0.65}Sr_{0.3}CoO_{3-\delta}$ is substantially higher than that of $NiCo_2O_4$, which is in agreement with literature data on dense ceramics and porous electrodes with a micron-scale grain

size.[1] The high electrochemical performance of the perovskite cobaltites is related to several factors including, in particular, higher electronic conductivity, weaker bonding between transition metal cations and oxygen or hydroxyl anions, and a wide range of possible oxygen-deficiency variations with respect to the spinel electrodes.[1,4,5]

Conclusions

The template synthesis of macroporous perovskite and spinel structures was successfully shown taking a macroporous block-copolymer gel as the template material. Resulting $La_{0.65}Sr_{0.3}CoO_{3-\delta}$ and $NiCo_2O_4$ networks exhibit a high surface area and inner structure similar to the porous structure of the initial template material. It was demonstrated that the templating method can be applied for the synthesis of porous inorganic materials at extremely high annealing temperatures above 1000 °C, which is necessary to form single perovskite or spinel crystal phases, resulting in macroporous inorganic replicas with a 20−50 nm particle size. Porous $NiCo_2O_4$ can be obtained employing both preformed $NiCo_2O_4$ sol and a precursor salt solution for impregnation of the template gel, while porous $La_{0.65}Sr_{0.3}CoO_{3-\delta}$ was formed only from preformed $La_{0.65}Sr_{0.3}CoO_{3-\delta}$ sol. Dense $La_{0.65}Sr_{0.3}CoO_{3-\delta}$ deposits were formed using precursor salt solutions for impregnation.

Macroporous $La_{0.65}Sr_{0.3}CoO_{3-\delta}$ and $NiCo_2O_4$ showed high electrocatalytic activity in oxygen electrooxidation reactions in an alkali water solution. The high activity is caused by high specific surface area of the samples, surface availability due to the macroporous structure, and high electrochemical performance inherent to these materials. Macroporous $La_{0.65}Sr_{0.3}CoO_{3-\delta}$ and $NiCo_2O_4$ may be of significant interest for applications in the electrochemical industry as perspective and stable anodes for electrolysis in alkaline electrolytes (e.g., copper refinement and iron production from alkaline ore solutions).

Acknowledgment. The work was supported by FCT, Portugal (Projects SFRH/BPD/18702/2004 and SFRH/BPD/11606/2002 and the POCTI program). The authors thank Dr. R. Caruso (University of Melbourne) for continuous support and stimulating discussions. D.S. acknowledges FP6 Marie-Curie Actions for an Individual Incoming Marie-Curie Fellowship.

CM050672U